

## Research papers

# Enhanced low flow prediction for water and environmental management

Santosh K. Aryal<sup>a,\*</sup>, Yongqiang Zhang<sup>b,\*</sup>, Francis Chiew<sup>a</sup>

<sup>a</sup> CSIRO Land and Water, Black Mountain, Canberra, ACT 2601, Australia

<sup>b</sup> Key Laboratory of Water Cycle and Related Land Surface Processes, Institute of Geographic Sciences and Natural Resources Research, Chinese Academy of Sciences, Beijing 100101, China

## ARTICLE INFO

This manuscript was handled by Marco Borga, Editor-in-Chief, with the assistance of Christian Massari, Associate Editor

### Keywords:

Low flow estimation  
Flow transformation  
Baseflow  
Cease-to-flow  
Zero flow days

## ABSTRACT

The ability to predict low river flows is critical to water resources planning to sustain a healthy river ecosystem. However, the estimation of reliable low flows is difficult for a variety of reasons including lack of its proper conceptualisation. Consequently, arbitrary flow data transformation is done to enhance the influence of lower flows to help improve the goodness-of-fit during parameter optimisation in rainfall-runoff modelling. We carried out systematic model calibration using a range of flow data transformations to identify the one that results in best goodness-of-fits in 595 catchments across different rainfall regions of Australia. Effects of transformation methods on the prediction of low flow surrogates, namely the Baseflow Index (BFI) and cease-to-flow days or the Zero Flow Days (ZFD) were also investigated and regionalised. We found that the square-root transformation performed the best in modelling flow time series in all rainfall regions of Australia and for different ranges of precipitation and forest cover. Model parameters from most flow transformations predicted the mean annual ZFD and mean annual BFI well. Parameters from the log- and reciprocal-transformed flow were best in estimating the annual ZFD, while square-root and no-transformation did well in predicting the annual BFI. The observed BFI and ZFD were strongly correlated with the mean annual precipitation at a 5% significance level in all regions. It is also the biggest influencing factor for ZFD and BFI among several catchment attributes. ZFD and BFI had a strong negative correlation with each other implying that they may be interchangeable as low flow surrogates. There was a clear and widespread reduction in the probability of baseflow occurrence during the Australian millennium droughts of 2001–2010. The probabilities were reduced by up to 70% compared to the before-drought baseflow probability.

## 1. Introduction

The ability to predict low river flows and connectivity to groundwater systems during dry periods is critical to river operations and water resources planning. Low flow is quite sensitive to human activities, like afforestation, deforestation, agriculture and extractive resource development (e.g. mining), which is compounded by climate change. Water metrics reflecting the entire range of river flow distribution are important to develop water plans to share water optimally between competing needs, especially when the water is scarce. Reliable low flow estimates inform environmental watering and water quality management to sustain healthy ecosystems. However, whilst hydrological models can generally simulate the medium- and high-flows reasonably well, accurate prediction of low flow remains a significant challenge (Nicolle et al., 2014). The low flow prediction is difficult everywhere because of lack of established techniques and, in some regions e.g. Australia, because of widely experienced semi-arid conditions

with a large majority of intermittent streams and the high runoff variability.

The definition of low flow is not universal and perhaps necessarily so, as it depends on local hydroclimatic and other catchment characteristics and the purpose of its use (Efstratiadis et al., 2014; Pushpalatha et al., 2012; Smakhtin, 2001). Generally, low flow has been defined as the flow of water in a stream during the drier period the year. Several low flow indicators including Mean Annual Flow (MAF) are adopted as an arbitrary upper bound of low flow. Various low flow indices are then expressed as a percentage of the MAF (Smakhtin, 2001). The absolute minimum flow has also been discussed ignoring the natural variability of streamflow in different regions (Aguilar and Polo, 2016). Caruso (2002) evaluated temporal and spatial patterns of extreme flows in New Zealand during a severe drought and used low flow as the Mean Annual 7-day Low Flow (MALF) and 7-day low flow with a return period of 10 years (7Q10). Durations of low flow below MALF and 7Q10 were also used as indices of low flow. Laaha and Blöschl

\* Corresponding authors.

E-mail addresses: [santosh.aryal@csiro.au](mailto:santosh.aryal@csiro.au) (S.K. Aryal), [zhangyq@igsnrr.ac.cn](mailto:zhangyq@igsnrr.ac.cn) (Y. Zhang).

(2006) used a flow that is exceeded 95% of days (Q95) as their low flow, whilst Hannaford and Marsh, (2006) used annual minimum 7 and 30-day mean flows and number of days below the 70th and 90th percentile flows as surrogates of low flows. In the UK, no flow abstraction below Q95 in all rivers was suggested implying that to be the minimum flow (Acreman et al., 2008). We note that all these low flow indicators will invariably result in flow values that are zero for Australian conditions where most of the streams are intermittent with some stream flowing for less than 30% of the time. Although zero flow may be taken as the lower bound of flow in intermittent and ephemeral streams (Smakhtin, 2001), this is unhelpful for environmental flow planning. Various other indicators e.g. one percentile flow or arbitrarily defined low flow and low flow days were used in a recent study examining the comparative effects of coal and coal seam gas development on the environment over the no development scenario (Aryal et al., 2018). In this study, together with low flow, we use runoff signatures: the Baseflow Index (BFI) and cease-to-flow or the Zero Flow Days (ZFD) as low flow surrogates (Zhang et al., 2018). Baseflow index is the ratio of total baseflow volume to total flow volume over a given period. Several indices of zero flows, e.g. period of consecutive zero flow days can be used as one of the indicators of stream ecosystem health (Larned et al., 2010).

Modelling of low flow has been tricky. Although flow transformations to reduce the influence of higher flows on calibration have been practised (Oudin et al., 2006), those transformations mostly have been arbitrary and without testing to see if the transformation is indeed most effective (e.g. Aryal et al., 2018; Chiew et al., 1993; Krause et al., 2005; Zhang et al., 2014). Pushpalatha et al. (2012) evaluated the criteria for simulating low flow using a range of transformations to find that the Nash-Sutcliffe Efficiency (NSE) based on inverse (reciprocal) transformation is better suited in 940 French catchments. Since a majority of streams are perennial, these transformations may not adequately characterise flow behaviour in regions with drier climate regimes, such as Australia. Therefore, we will use six transformations to test their suitability and evaluate the best in rainfall regions across Australia.

Ecologists have sought the information on several low flow indicators e.g., the number of dry spells in streams as those play a major role in breeding and survival activities of invertebrates and other water-dependent species including fish, frogs, turtles and waterbirds together with supporting the riverine flora and its ecosystems (Rolls et al., 2012; Sheldon, 2017; Stromberg et al., 2007). Furthermore, effects of environmental changes on low flow, e.g. baseflow, are uncertain (Brown et al., 2013; Hamel et al., 2017). Price (2011) synthesised global literature investigating the relationship between baseflow and catchment characteristics concluding that the understanding of catchment characteristics on baseflow still remains to be resolved thus underscoring the need for further research.

Therefore, this research aims to enhance low flow prediction capability, through understanding and knowledge of the processes influencing low-flow and its surrogates by adapting hydrological models and data transformation, and testing the models results against streamflow data from 595 catchments across Australia. The focus is to study the behaviour of low flow and its surrogates to elucidate its key drivers and the causative factors. The evidence-based low flow predictions will allow policymakers and water managers to make more informed decisions on water sharing e.g. in river basin plans and water infrastructure development, impact of resource development on water-dependent assets (e.g. coal and coal seam gas development) and river operations for environmental watering. We ask the following questions (i) how to calibrate a model for low flow and what data transformation gives the best fit to observed low flows and its surrogates? (ii) does the best transformation vary from region to region? (iii) how effective is the regionalisation of the low flow modelling for estimating low flow or its surrogates in catchments with no observed data? (iv) how do catchment characteristics and hydro-climatic properties influence low flow and including baseflow and cease-to-flow events? and (v) can we link the

hydroclimatic characteristics, catchment morphology and vegetation to the transformation type? We also test our contention that lower flow characteristics vary from region to region and a single definition of low flow is neither possible nor meaningful.

The overall objective is to enhance hydrological modelling skills in predicting low flow metrics for each rainfall regions, for estimation of low flow and its surrogates across Australia, to ground the technique behind the low flow modelling to evidence-based knowledge.

The specific objectives include:

- (a) applying six data transformations and explore their performance in modelling low flow and its surrogates;
- (b) investigating the potential of parameter regionalisation for estimating low flow and its surrogate;
- (c) exploring and quantifying effects of drought on low flow behaviour; and
- (d) investigating how the flow surrogates, hydroclimate variables and catchment characteristics are correlated.

The next section describes the area and data used in this study. Section 3 describes the methods used to investigate low flow characteristics and modelling. The results are provided in Section 4 followed by discussion and conclusion in sections 5 and 6 respectively.

## 2. Study area and data

Daily streamflow, precipitation, evaporation and forest cover and other data of 595 catchments ranging from 50 to 4806 km<sup>2</sup> (median 346 km<sup>2</sup>) are available (Fig. 1). These are a subset of 780 unregulated and unimpaired Australian catchments not subjected to major diversion or irrigation (<https://publications.csiro.au/rpr/pub?pid=csiro:EP113194>). Ninety-five per cent of selected catchments have 4.1% or less irrigated area and more than 80% have less than 1% area under any irrigation. The flow data ranges from 1975 to 2012 with different extents of data gaps. These catchments are distributed in four rainfall regions: arid, tropics, winter and equiseasonal comprising 37, 83, 90 and 385 catchments respectively. The regions represent arid to temperate as well as tropical and Mediterranean climates with Mean Annual Precipitation (MAP) of 530 mm, 1465 mm, 973 mm and 763 mm respectively.

During 2001 to 2009 much of south-eastern Australia experienced a prolonged dry condition, known as the Millennium Drought that severely affected catchments runoff in the Murray-Darling Basin (Australian Bureau of Meteorology, 2015).

## 3. Methods

### 3.1. Low flow and its surrogates

The model's ability to simulate low flow and its surrogates was tested by using a range of data transformations to enhance the lower flows and dampen the higher flows to different extents. The baseflow and zero flow days were determined as described below.

#### 3.1.1. Baseflow separation and calculation of baseflow index

Among many baseflow filters, Chapman (1999) found the use of one- and three-parameter filter leads to implausible results given by unrealistic base flow index and the baseflow hydrograph shape. Accordingly, we used the two-parameter filter by Eckhardt (2005) as proposed by Bates and Aryal (2014):

$$Q_b(k) = [a(1 - b\max)Q_b(k - 1) + b\max(1 - a)y(k)]/(1 - ab\max) \quad (1)$$

subject to

$$Q_b(1) = y(1) \quad (1a)$$

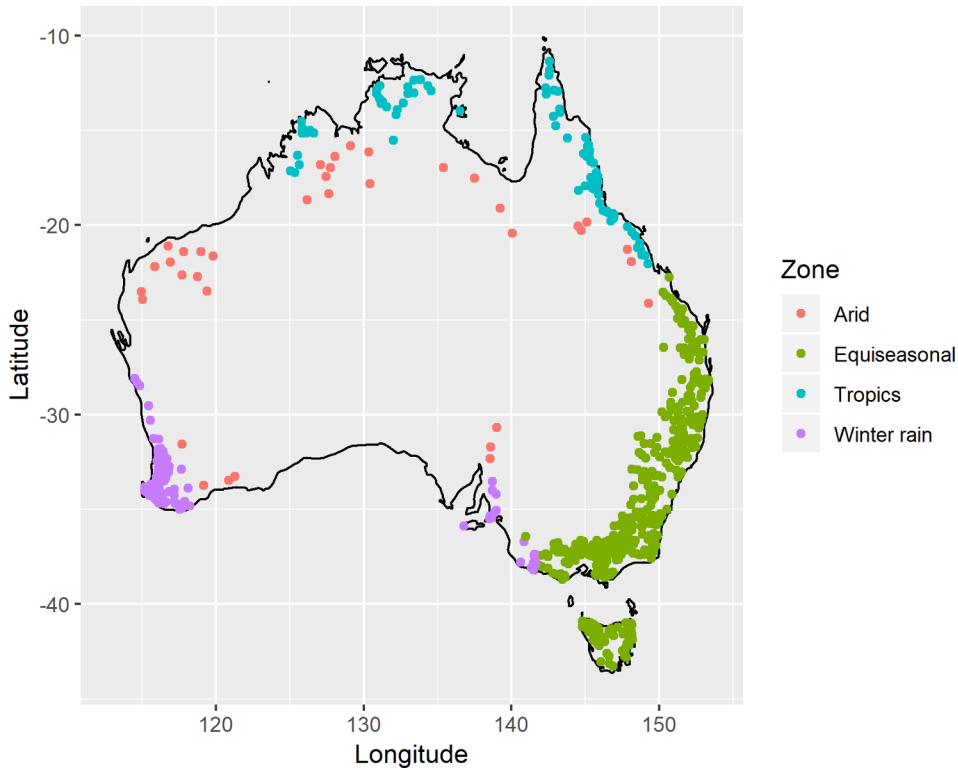


**Fig. 1.** Distribution of 595 catchments across Australia used in the study.

$$Q_b(t) \leq y(t) \quad (1b)$$

where  $Q_b$  is the baseflow (mm/d),  $y_k$  is total streamflow (mm/d) in time  $t$  (d),  $\alpha$  is the baseflow recession constant (1/d),  $b_{max}$  is the maximum value of the BFI (-) that can be produced by the filter and  $k$  is the number of ordinates in the storm hydrograph of interest. The maximum value of baseflow index  $b_{max}$  is not an easy parameter to estimate and generally guesswork is applied based on catchment characteristics (Zhang et al., 2017). In this study, we used  $b_{max}$  values calculated using the baseflows derived from the one-parameter filter (Lyne and Hollick, 1979) given by:

$$Q_b(k) = \alpha Q_b(k-1) + (1-\alpha)(y(k) + y(k-1))/2 \quad (2)$$

subject to 1a and 1b.

The baseflow recession constant is determined for each of the 595 catchments using the observed data using a method by Eckhardt (2008). The daily streamflow data  $y_k$  which forms a part of the recession period for at least five days is considered, such that

$$y_{k-3} > y_{k-2} > y_{k-1} > y_k > y_{k+1} > y_{k+2} \quad (3)$$

Eckhardt (2008) considers if the above were long enough the streamflow would consist entirely of baseflow. If there is no groundwater recharge and assuming linear reservoir:

$$y_{k+1} = \alpha y_k \quad (4)$$

where  $\alpha$  is the baseflow recession constant used in Eq. (1).

### 3.1.2. Zero flow days

Calculation of zero flow (cease-to-flow) days is non-trivial due to the asymptotic nature of streamflow cessation resulting in near-zero flow for extended periods. Depending on the catchment size, nature of flow and measurement limits of the streamflow gauge, the amount that can be considered the zero flow can vary (Smakhtin, 2001). The zero flow days are calculated using a staged process which assigned flow below a low threshold to zero flows depending on values of other observed flows. Using trial and error, this threshold was gradually increased up

to 0.5 mm. Any stream with greater than 0.5 mm runoff for the whole year is taken as perennial for that year. This criterion is also adequate to evaluate hydrological model performance since there exists large uncertainty in hydrological models, such as GR4J to simulate streamflow that approaches zero flow (Zhang et al., 2014).

### 3.1.3. Effects of droughts on probability of baseflow

In areas where baseflows have been sustained by regional groundwater or shallow aquifers, prolonged absence of precipitation causes disconnection between groundwater and river channels resulting in cessation of the baseflow. Flow Duration Curves (FDC) of baseflow during the Australian Millennium Drought of 2001–2010 (see Australian Bureau of Meteorology (2015) for the extent of the drought) were compared with FDCs of that before the drought to determine the difference in the probability of any baseflow caused by the drought.

### 3.2. Hydrological model calibration

We used the GR4J daily lumped conceptual rainfall-runoff model (Perrin et al., 2003). It is a four-parameter ( $x_1$ ,  $x_2$ ,  $x_3$ ,  $x_4$ ) model widely used under a variety of conditions (e.g. Coron et al., 2012; Li et al., 2013; Nepal et al., 2017). The model uses precipitation and potential evapotranspiration depths (mm) as inputs. It consists of two main storages: the production store and the routing store (Fig. S1). Parameter  $x_1$  is the maximum capacity of the production store (mm);  $x_2$  determines the flux to/from groundwater (mm);  $x_3$  is the maximum capacity of the routing store (mm);  $x_4$  controls the recession of the unit hydrograph (day). Low flow in GR4J is generated by the percolation from the production store (S), outflow from the routing store (R) and the groundwater exchange function (F) which either imports water from or export water to the surrounding aquifers (Pushpalatha et al., 2012).

Model calibrations are carried out using untransformed flow and six sets of flow transformations. Those are (i) log10 transform (ii) inverse (reciprocal) transform, and (iii) to vi power transformations using

$\frac{1}{20}$ , 1/10, 1/5 and 1/2 (0.05, 0.1, 0.2 and 0.5 respectively) exponents. Log and inverse transforms used a small error term to handle zero flows. The optimisations were done using the modified Kling-Gupta Efficiency (KGE) (Gupta et al., 2009; Kling et al., 2012) goodness-of-fit calculated using transformed values of both the observed and simulated flows for each of the six transformations. The KGE overcomes shortcomings of the widely used NSE criterion using correlation coefficient between observed and simulated runoff ( $r$ ), bias ( $\beta$ ) and variability ratio ( $\gamma$ ) (Schaeefli and Gupta, 2007). The ideal value of Modified KGE (MKGE) is 1. NSE and Percentage Bias (PBIAS) values were also calculated. Appendix A gives formulations for MKGE, NSE and PBIAS. A global optimiser, the Shuffled Complex Evolution (SCE-UA) (Duan et al., 1994) was used for parameter optimisation. The SCE-UA approach treats the global search as a process of natural evolution. In this, the number of sample population is divided into several complexes, each of which is allowed to search in different directions. These are then mixed and new complexes are formed through shuffling (Duan et al., 1994). Each point of a complex is a potential parent and varying combinations of these points produce offspring in every complex (Duan et al., 1994; Eckhardt and Arnold, 2001). To ensure that the evolution process is competitive and better parents contribute to the generation of offspring, the points of lower fitness are replaced by better offsprings. The global optimum is obtained by new points created in the feasible parameter space through ‘mutation’ and recombination of the points into new complexes (the shuffling) (Duan et al., 1994; Eckhardt and Arnold, 2001).

Regionalisation of model parameters for estimation of low flow time series, ZFD and BFI is explored based on comparison of observed values with simulated values using the optimised donor parameters from single nearest neighbour catchments (Burn and Boorman, 1993; Parajka et al., 2005; Zhang et al., 2014), and from catchments considered ‘similar’ based on physical similarity criteria (Zhang and Chiew, 2009). The nearest neighbour is chosen based on the shortest Euclidian distance between two catchments’ centroids, while three separate rank-accumulated similarity criteria are evaluated to determine the similar catchments. Catchment attributes used as causative variables in this study are: MAP, mean annual Potential Evaporation (PET), catchment area, forest cover and slope. These attributes are also used in the causality analysis (Section 3.3). For each attribute, the catchment with closest attribute value is considered ranked one. To determine similar catchments for donor parameters, catchments are ranked by (i) the aridity index (PET/MAP) (ii) all causative variables with separate weight assigned to each based on the regression coefficients in Table 1, and (iii) all causative variable with equal weight assigned each (Zhang and Chiew, 2009). Donor catchments determined from all three physical similarity criteria are used in the regionalisation.

Model evaluations are done using the MKGE. The NSE and PBIAS are also used to judge the model’s performance using on-site and regionalised parameters. The model performance in terms of the two low flow surrogates is tested using values derived from the observed and simulated flow time series. We did not recalibrate the model using annual ZFD and BFI as those from transformed flows are not physically meaningful.

### 3.3. Causality analysis

#### 3.3.1. Correlations

The correlation and covariance among ZFD, BFI, mean annual precipitation, mean annual potential evaporation, catchment area,

forest cover and slope are evaluated for the whole of Australia and each of its rainfall regions. Shapiro-Wilk test (Shapiro and Wilk, 1965) and normal quantile-quantile plots are used to test the normality of these variables. For data that do not follow the assumption of normality, the Spearman rank correlation can be used (Merz and Blöschl, 2009), which gives a nonparametric measure of statistical dependence of variables without the assumption of data being normally distributed (Hauke and Kossowski, 2011). The Spearman rank correlation coefficient ( $\rho$ ) is given by Corder and Foreman, (2009):

$$\rho = 1 - \frac{6 \sum D_i^2}{n(n^2 - 1)} \quad (5)$$

where  $D_i$  is the difference between each pair of the ranked variables ( $X_i - Y_i$ ) and  $n$  is the number of ranked pair samples (Xiao et al., 2016). Relationships for data with ties in ranks are different from Eq. (5) (Cleff, 2014).

#### 3.3.2. Multiple linear regression

In addition to one-to-one correlation, regression relationship is established using the multiple linear regression to test the predictability of the two independent variables (BFI and ZFD) by combining their most likely causative drivers (De Vera, 1984; McIntyre et al., 2007). Past researchers have used linear regression to quantify a range of catchment characteristics on the baseflow index (Bloomfield et al., 2009; Lacey and Grayson, 1998; Zhang et al., 2013). The general model for multiple linear regression that relates dependent variable  $y$  to independent variables  $x$ ’s is given by

$$y = \beta_0 + \beta_1 x_1 + \beta_2 x_2 + \dots + \beta_n x_n \quad (6)$$

where  $\beta_0$  is the intercept and  $\beta_1, \beta_2, \dots, \beta_n$  are the regression coefficients associated with  $x_1, x_2, \dots, x_n$  respectively. Although it is possible that relationships may be non-linear, we did not have a way of knowing the form of non-linearity.

## 4. Results

### 4.1. Temporal and spatial patterns of baseflow and low flows across Australia

Preliminary data analysis was done to investigate the characteristics of observed baseflow and zero flow days. The distribution of mean annual BFIs across Australia generally showed lower BFIs in semi-arid (most catchments of the Pilbara region in northwest Western Australia) and inland regions (Fig. 2a) compared to coastal areas of south-east Victoria, whole of Tasmania, tropical north Queensland and south-west of Western Australia. Similarly, arid regions of the Australian interior and semi-arid Pilbara region have mean annual ZFDs greater than 300 days. Streams in Tasmania, northern tropical regions and in east coast regions have much smaller ZFDs (Fig. 2b).

### 4.2. Effect of the millennium drought on the baseflow

The reduction in probability of baseflow correlated well with the extent of drought across Australia during the Millennium Drought of 2001–2010. The flow duration curves for periods before and during the drought in the affected area, containing 333 of 595 catchments (Australian Bureau of Meteorology, 2015), were analysed. They showed that greater than 80% of those catchments experienced a reduction in

Table 1

Coefficients,  $R^2$  and p-values of the multiple linear regression among ZFD/BFI and mean-normalised causative variables.

Variable y	$B_1$ (Area)	$\beta_2$ (MAP)	$\beta_3$ (PET)	$\beta_4$ (Forest Cover)	$\beta_5$ (Slope)	$\beta_0$ Intercept	Coefficient of determination $R^2$	p-value
ZFD	-1.5	-88.2	31.5	-74.0	-25.0	261.3	0.58	<<0.01
BFI	0.02	0.10	-0.14	0.11	-0.006	0.57	0.30	<<0.01

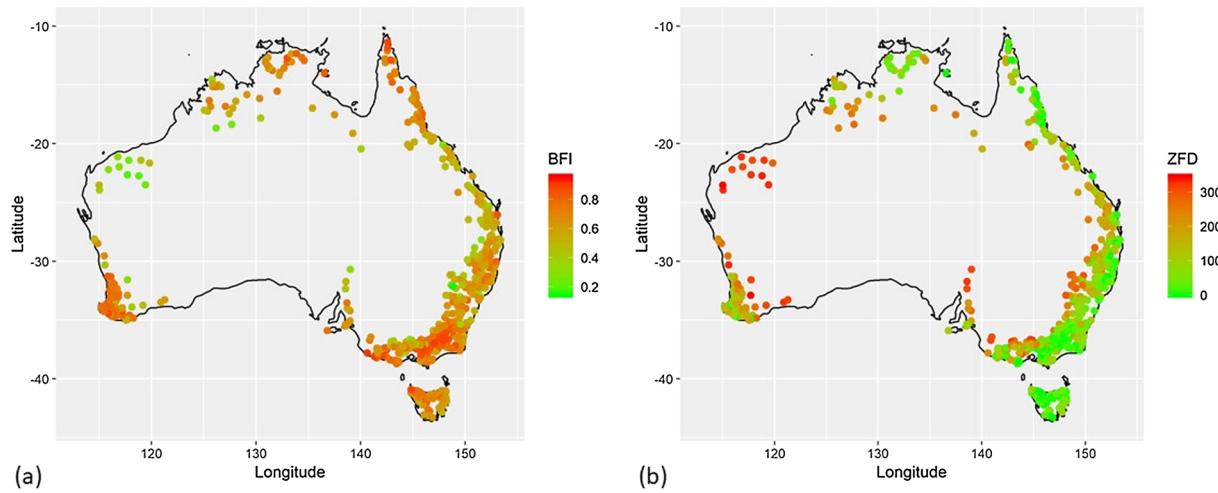


**Fig. 2.** Distribution of (a) mean annual BFI and (b) mean annual ZFD across Australia.

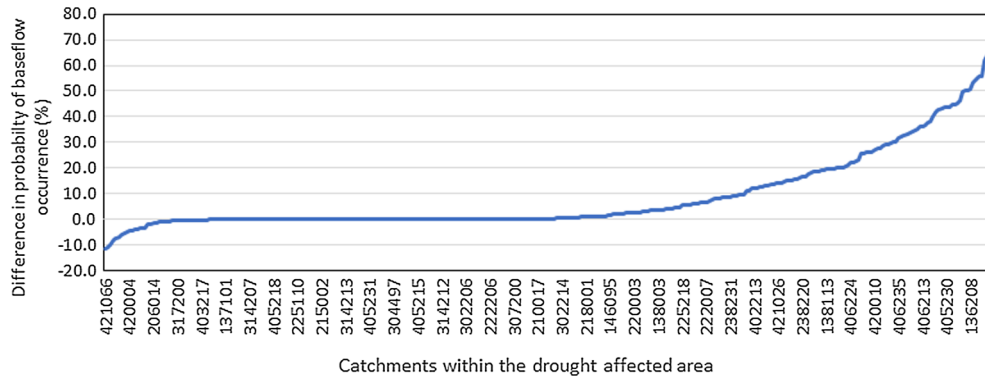


**Fig. 3.** Difference in the probability of any baseflow before and during the Millennium Drought. A positive value indicates the reduction in probability during the drought. The probability curve (blue line) contains data from all 333 drought-affected catchments, however, the x-axis is labelled with only a fraction of those catchments for clarity.

the probability of any occurrence of baseflow (Fig. 3). More than 10% of the catchments showed greater than 30% reduction in the probability of baseflow. For example, for Barker Creek catchment in Queensland (136208), the probability of any baseflow reduced from about 80% to 10% (Fig. 3).

#### 4.3. Causality analysis

##### 4.3.1. Correlation of annual ZFD and BFI to other catchment attributes

Correlations among all causative and dependent variables were investigated (Fig. 4). The Spearman's rho ( $\rho$ ) and p values show that ZFD is correlated with precipitation ( $-0.7$ ) and PET (0.29) at a 5% significance level ( $p < 0.01$ ). Overall, the ZFD was also negatively well correlated with slope ( $\rho = -0.6$ ,  $p < 0.01$ ) however, no significant correlations between slope and ZFD were found in arid and winter rainfall zones (Fig. 4). Precipitation, PET and forest cover were correlated well with ZFD at a 5% significance level across all rainfall regions. The catchment area, however, had no correlation with ZFD in the arid region but had a weak ( $\rho = 0.13$ ) but statistically significant correlation in the eiseasonal rainfall region. A better correlation between ZFD and catchment area was found in the other two regions. Good correlation also existed between forest cover and both the ZFD ( $\rho = -0.6$ ) and BFI ( $\rho = 0.45$ ).

The BFI was positively correlated to precipitation and negatively correlated to the PET. Catchment area had no statistically significant correlation with BFI in any of the rainfall regions. BFI also had a strong and statistically significant positive correlation ( $p < 0.01$ ) with precipitation in all rainfall regions. The BFI, however, had no statistically significant correlation with PET in all regions except the eiseasonal rainfall region, where it was negatively correlated ( $\rho = -0.36$ ). BFI

had a good and statistically significant correlation with forest cover in all but the tropics region. The ZFD and BFI were also strongly negatively correlated ( $\rho = -0.57$ ) at 5% significance level for the whole of Australia (Fig. 4) as well as for each of the rainfall regions (Fig. 5). These results are interpreted in the discussion section.

##### 4.3.2. Regression relationships between ZFD, BFI and other variables

The functional relationship between ZFD and BFI, and mean-normalised causative variables using multiple linear regression showed that MAP, PET and forest cover had a reasonable and statistically significant influence ( $p \ll 0.01$ ) on ZFD (Table 1). The catchment area, however, has almost no influence on ZFD in combination with other variables. The BFI also shows a similar dependence on these variables but with a smaller  $R^2$ . It is difficult to compare these results with those from earlier studies because of the different variables used in different studies.

#### 4.4. Best transformation to model low flow

##### 4.4.1. Onsite calibrated parameters

Comparison of goodness-of-fit values showed that the square-root transformation had the highest range of MKGE calculated using transformed values of both the observed and simulated flow series for 595 catchments (Fig. 6a, Table 2). Among all transformations, the winter rainfall region had the highest median MKGE and the arid had the lowest. The square-root transformation produced the best MKGE also for different levels of forest cover and annual precipitation (Fig. 6 b, c). As expected, MKGE values for all transformations are generally well correlated to each other at a 0.05 significance level (Fig. S2). Correlation of MKGE between no-transformation and the reciprocal

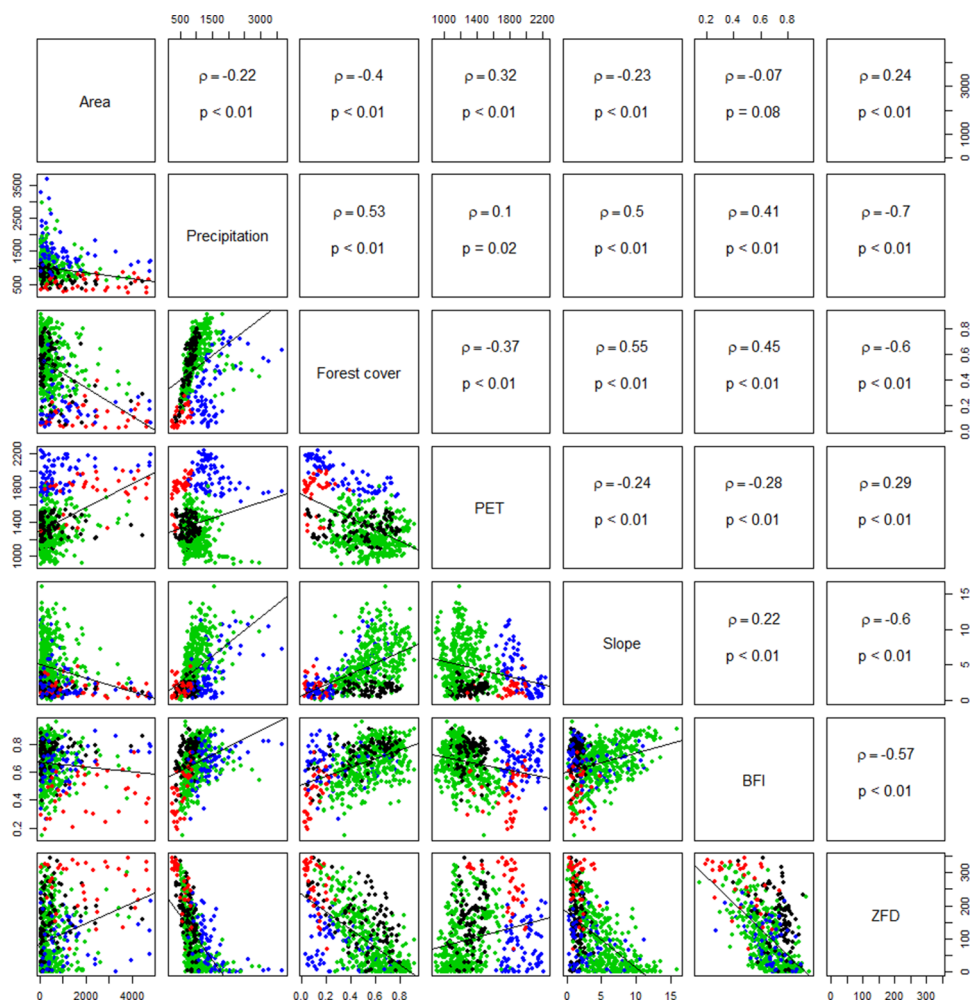


**Fig. 4.** Correlation among all causative and dependent variables. The different colours show points for different rainfall regions (red = arid; green = equiseasonal; blue = tropics; black = winter rainfall).  $\rho$  and  $p$  are the Spearman's rho and  $p$  values respectively.

transformation was the weakest ( $\rho = 0.24$ ), while the one-fifth and one-tenth transformations had the strongest correlation ( $r = 0.93$ ). The square-root transformation also resulted in best NSE (0.77) and nearly the best PBIAS (0.6).

#### 4.4.2. Regionalised parameters

Of three physical similarity criteria, donor parameters from the first two resulted in worse goodness-of-fit (MKGE) for simulating the flows than the one that assigned equal weight to all attributes. Consequently, further results of only the best performing similarity donor are presented here. Unsurprisingly, all the goodness-of-fit indicators using parameters from both the nearest neighbour donor and similarity-based donor catchments were generally worse than those obtained from the on-site calibrated parameters (Fig. 7, Table 2).

#### 4.5. Best transformation for low flow surrogates

##### 4.5.1. Zero flow days estimation

Annual ZFD values were estimated for all 595 catchments using observed and simulated flow series for all transformations using onsite calibrated parameters. Reciprocal and log transformations resulted in the better range of MKGE and NSE for annual ZFD values across Australia (Fig. 8a, b) suggesting their use for investigating maximum and minimum ZFD in any given catchment.

The log transformation resulted in the best overall estimation of simulated long-term mean annual ZFDs with MKGE and NSE of 0.95

and 0.97 respectively (Table 3). The performance of square-root and reciprocal transformations were mixed in terms of MKGE and NSE as the second and third alternatives. Square-root and log transformations resulted in better PBIAS values than the other transformations. The model calibration using one-tenth data transformation resulted in the worst overall MKGE (0.56) and NSE (0.60) and PBIAS ( $-40.8$ ) for ZFD estimation using onsite calibrated parameters.

Scatterplots of observed and simulated mean annual ZFDs depict their range across different rainfall regions (Fig. 9) and the modelling performance. For different rainfall regions, log, reciprocal and square-root transformations gave a mix results for the best MKGE and NSE values (Tables 4 and 5).

##### 4.5.2. ZFD regionalisation

For all modelling, the goodness-of-fit indicators obtained using the regionalised parameters were worse than those using the onsite-calibrated parameters. However, the MKGE values from regionalised parameters were greater than 0.6 for all except one-tenth transformation (Table 3). Scatterplots of observed and simulated ZFD values using donor parameters from the nearest neighbour (Fig. 10a–f) and similarity criteria (Fig. 10g–l) show performance slightly better than the former. MKGE, NSE and PBIAS values using data derived from the regression equation in Table 1 were better than or comparable to those obtained from simulated regionalised parameters (Table 3). Like the onsite calibrated parameters, the nearest neighbour and similarity-based donor parameters also resulted in better MKGE values in most

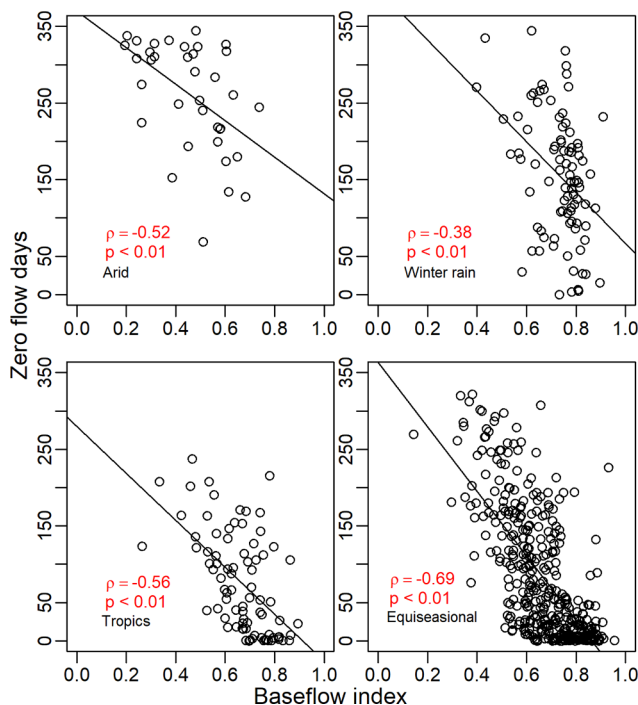


**Fig. 5.** Correlation between BFI and ZFDs in different rainfall regions across Australia. The straight line shows the linear model fit.  $\rho$  and  $p$  are the Spearman's rho and  $p$  values respectively.

rainfall zones for log, reciprocal and square-root transformations (Table 4). NSE values were mostly good for equiseasonal region using both two sets of donor parameters, while they were much worse for the tropics region; the rest had mixed results (Table 5). Less than 10% PBIAS was observed in nearly all regions using the onsite and nearest neighbour donor parameters. The similarity-based donor parameters performed worse than those two in all except the arid region (Table S1).

#### 4.5.3. Baseflow index estimation

Annual BFI values for all transformations were estimated using the observed and simulated flow series. The square-root and no-transformations resulted in the best range of MKGE for annual BFI values in all catchments (Fig. S3). Log and no-transformation produced the best overall estimation of simulated mean annual BFIs with MKGE of 0.84 (Table 6). The model calibration using one-tenth data transform resulted in the worst overall MKGE (0.17).

Scatterplots of observed and simulated mean annual BFIs show their value range across different rainfall regions (Fig. 11). For the four rainfall regions, three different transformations resulted in best MKGE for mean annual BFIs (Table 7). The MKGEs were much better than the NSEs (Table 8).

#### 4.5.4. BFI regionalisation

For the whole of Australia generally, MKGE values were better than NSE values from both the nearest neighbour and similarity-based donor parameters and were much closer to those from the onsite calibration (Table 6). The nearest neighbour parameters produced mixed results in terms of MKGE and NSE values for different transformation techniques depending on the rainfall regions (Table 7, Table 8). The similarity-based donor parameters also had a mixed performance depending on the rainfall region and their performance was also consistently worse than the nearest neighbour parameters. The MKGE from BFI derived from the regression relationship in Table 1, was lower than those from the donor parameters. The NSE and PBIAS values, however, were better than or comparable to those obtained from regionalised parameters (Table 6).

## 5. Discussion

Low flow modelling has not been given the importance it deserves. Despite ongoing hydrological research, knowledge of techniques for low flow estimation is rather limited. Generally, modelling for low flow estimation is based on calibration using overall streamflow hydrographs and optimising on goodness-of-fit indicators (e.g. NSE) that are biased towards higher flows (McCuen et al., 2006; Staudinger et al., 2011). On occasions when flow transformations are used to reduce the influence of higher flow on model calibration (Oudin et al., 2006), they mostly have been arbitrary. This is because limited research has tested the effectiveness of each transformation (e.g. Pushpalatha et al., 2012), leading to no dependable method to model the low flow and its surrogates, potentially leading to suboptimal low flow estimation (e.g. Aryal et al., 2018; Chiew et al., 1993; Zhang et al., 2014).

The optimal low flow estimation is also hampered by the lack of a proper definition of low flow as it depends on local hydroclimatic and other catchment characteristics, and the purpose of its use. Low flow definition focussed on a given percentage of observed flows is not uniformly useful to all regions as it assigns different flow amounts in different catchments. Since the interest in low flow is not in its universal absolute or relative value but is in the existence of a minimum flow that serves a purpose for a riverine environment e.g. sustaining the crucial local stream ecosystem or fulfilling a consumptive or non-consumptive use demand. It may well also depend on how much flow (or extent of no flow) a given species within the ecosystem needs to survive. Therefore, together with low flow, we also studied estimation of its surrogates e.g. cease-to-flow days that the ecologists are interested in to evaluate the survival of stream ecosystems. Since ZFD or the length of dry spells are critical to understanding the ecological health of the streams, we investigated whether the flow transformations that provided better goodness-of-fit values were also better at estimating low flow surrogates? As discussed earlier, the threshold below which the flow is considered as zero varies from catchment to catchment, therefore the estimation of ZFDs was not straightforward and had to be determined through an iterative process as described in Section 3.1.2.

The ZFD had good and statistically significant correlations with catchment area, forest cover, slope, PET and precipitation confirming that low flow characteristics vary from region to region and a single definition of low flow is neither possible nor meaningful. The performance of different transformations for estimating annual low flow surrogates revealed that log, reciprocal and square-root transformations can be considered best as shown by the central tendencies (mean or median) of goodness-of-fit values. One-tenth or lower transformations performed the worst. This, interestingly, suggests that the optimum flow calibration using a given transformation does not necessarily result in a corresponding better estimation of low flow surrogates. Therefore, a few flow transformation techniques must be tested to ensure that crucial low flow surrogates are correctly estimated.

Pushpalatha et al. (2012) advised against using non-transformed flow for evaluating low flows and suggested the use of reciprocal transform based on their study in the French catchments. We found that the square-root transformation provided better goodness-of-fit in Australian streams than any other. The non-transformed flow was better in simulating low flow surrogates, especially the mean annual BFI, than a 1/10th (or less) power transformed flow. This is because the BFI may also contain some medium flows ensued after a rainfall storm. Most transformations, except very low order transformations, were useful in predicting mean annual zero flow days and baseflow index.

We found that nearest neighbour parameters performed reasonably well in estimating low flow and its surrogates. Their performance, however, varied from region-to-region and transformation-to-transformation, especially for the surrogates. The parameters from physical similarity-based donor catchments consistently performed worse than those from nearest neighbours. Regionalisation using nearest neighbours have been used with mixed results elsewhere. For example, Merz

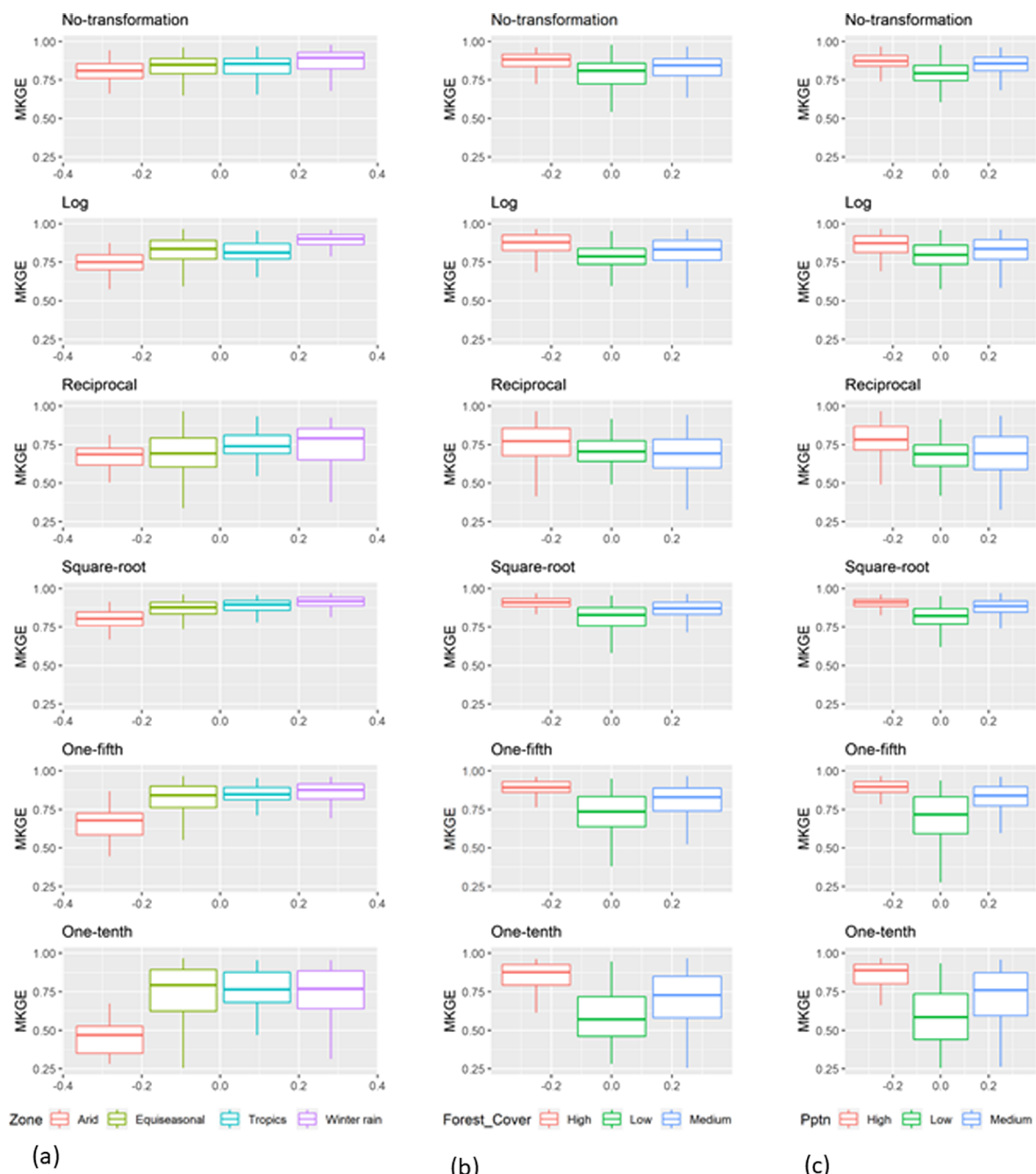


**Fig. 6.** Range of optimised MKGE for different transformations for different (a) rainfall regions (b) level of forest cover and (c) mean annual precipitation. Results for 1/20 transformation is not shown. The whiskers show 1.5 times the interquartile range.

**Table 2**

Median MKGE, NSE and PBIAS of simulated flow for different data transformations using onsite-calibrated (OS), nearest neighbour donor (NN), and similarity-based donor (SD) parameters. The goodness-of-fit is calculated using transformed values of both the observed and simulated flows.

Transformations	MKGE			NSE			PBIAS		
	OS	NN	SD	OS	NN	SD	OS	NN	SD
No-transformation	0.85	0.59	0.44	0.72	0.54	0.45	0.5	2.3	2.4
Log	0.84	0.65	0.59	0.72	0.53	0.46	2.2	4.9	4.7
Reciprocal	0.71	0.41	0.32	0.57	0.23	0.10	2.2	9.0	-0.6
Square-root	0.88	0.67	0.58	0.77	0.65	0.57	0.6	-0.9	2.7
One-fifth	0.84	0.63	0.58	0.71	0.53	0.44	1.6	0.7	3.5
One-tenth	0.75	0.52	0.45	0.51	0.29	0.22	3.1	1.3	2.6

and Blöschl (2004) found spatial proximity to be better for regionalisation than those dependent on catchment attributes. Chiew and Suriwardena (2005) also found that parameters from nearest neighbour performed consistently better than those estimated from regionalisation relationships. Furthermore, Zhang and Chiew (2009) also found that the nearest neighbour donors performed slightly better than those from the physical similarity approach. In another study, Zhang et al. (2014) compared the nearest neighbour method with three other spatial interpolation methods: kriging, spline and inverse distance weighting (IDW) and found that nearest neighbour had a mixed performance for predicting hydrological indicators. It is noted, however, that nearest neighbour with very different catchment and hydroclimatic attributes may not follow this rule (Li et al., 2010). Although modelling gives the needed flow time series, we found that the mean annual ZFD and BFI

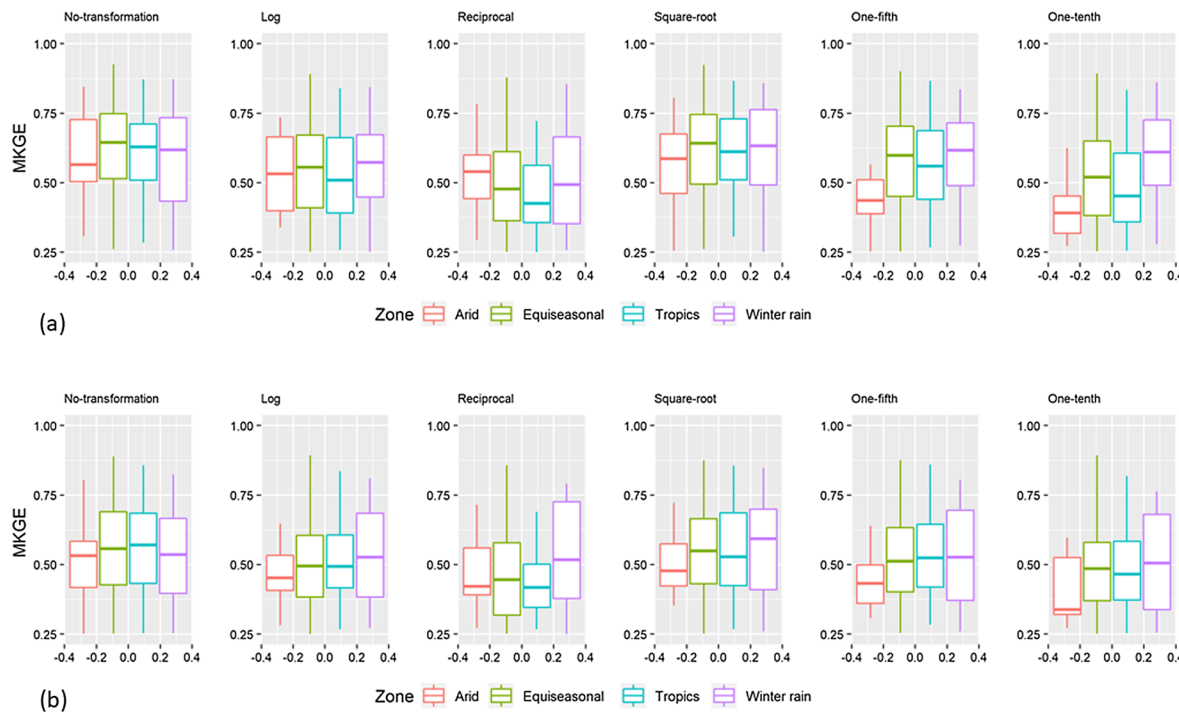


**Fig. 7.** Range of MKGE for flows simulated using donor parameters from (a) the nearest neighbour catchments, and (b) catchments selected based on the physical similarity criteria. The whiskers show 1.5 times the interquartile range.

estimations using regression relations based on causative variables were better than those obtained from one-tenth flow transformation using onsite calibrated parameters. Furthermore, the performance of regression relationships in estimating mean annual ZFD and BFI values was comparable to, or better than those of the nearest neighbour or physically similarity-based regionalisation techniques indicating the importance of such estimations in regionalisation.

The strong correlation between BFI and ZFD for the whole of Australia as well as for each rainfall regions suggests that either of these two surrogates can be used to estimate the other. As the ZFD can be determined from the observed streamflow data, it can be used to estimate the BFI which is harder to determine. As expected, BFI and ZFD also have a strong negative and positive correlation respectively with precipitation. However, both of those also had a statistically significant negative and positive correlation with the slope. Most of this correlation was dominated by the catchments in the equiseasonal rainfall region

including the hilly Tasmanian catchments (Fig. 1) with lower ZFDs (Fig. 2a). The opposite applies to the BFI.

The determination of the cease-to-flow days is subjective as it depends on several factors (e.g. accuracy of flow gauge at the lower scale) which vary from catchment to catchment, and therefore, is harder to tract. Although its determination can have a marginal quantitative effect on our results, our overall qualitative findings should be robust, since based on the modelling and observation in Australian catchments from a wide range of climates and rainfall regions. These regions vary from arid to temperate and include tropical and Mediterranean (south-west Western Australia) climates and rainfall regions. Since the low flow modelling is investigated for each of these regions, these findings should be transferrable to other geographies across the world.

Finally, our study investigates flow transformation methods for model parameter estimation geared towards the simulation of ‘lower’ flows and identifies one that produces best goodness-of-fit. Each of

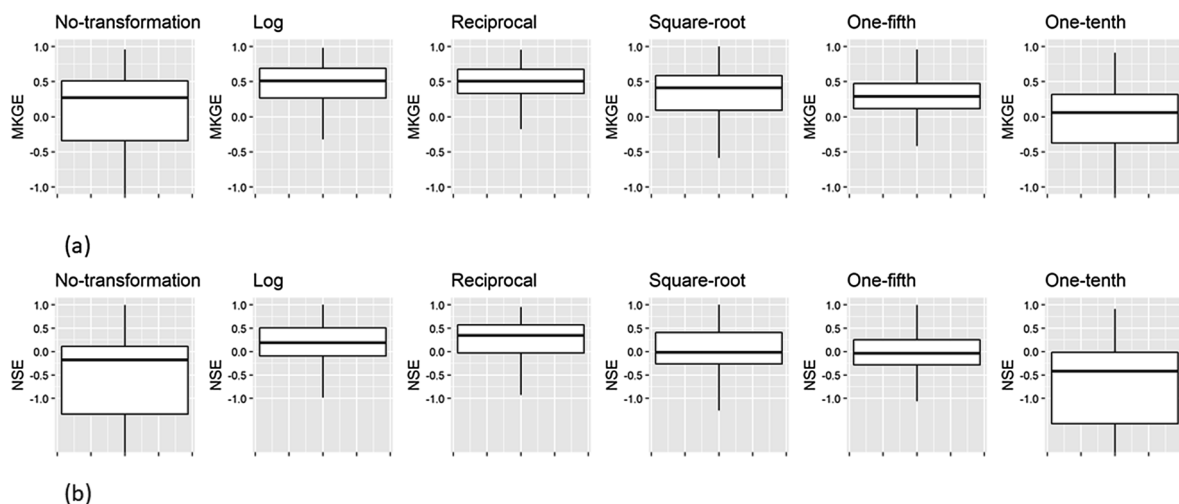


**Fig. 8.** Range of (a) MKGE and (b) NSE for simulated annual ZFD. The whiskers show 1.5 times the interquartile range.

**Table 3**

MKGE, NSE and PBIAS of simulated mean annual ZFD for different data transformations using onsite-calibrated (OS), nearest neighbour (NN) and similarity-based donor (SD) parameters. MKGE, NSE and PBIAS of ZFD values derived from the regression equation are also shown.

Transformations	MKGE			NSE			PBIAS		
	OS	NN	SD	OS	NN	SD	OS	NN	SD
No-transformation	0.78	0.64	0.68	0.64	0.41	0.40	10.4	16.3	4.0
Log	0.95	0.78	0.77	0.97	0.59	0.55	3.6	7.4	0.1
Reciprocal	0.89	0.79	0.73	0.95	0.57	0.45	-10.6	-6.1	-14.5
Square-root	0.92	0.75	0.77	0.92	0.56	0.53	2.3	7.5	-3.1
One-fifth	0.80	0.73	0.67	0.88	0.47	0.41	-19.8	-15.5	-23.1
One-tenth	0.56	0.53	0.46	0.60	0.24	0.12	-40.8	-37.6	-43.9
Regression Equation					0.60				-2.48

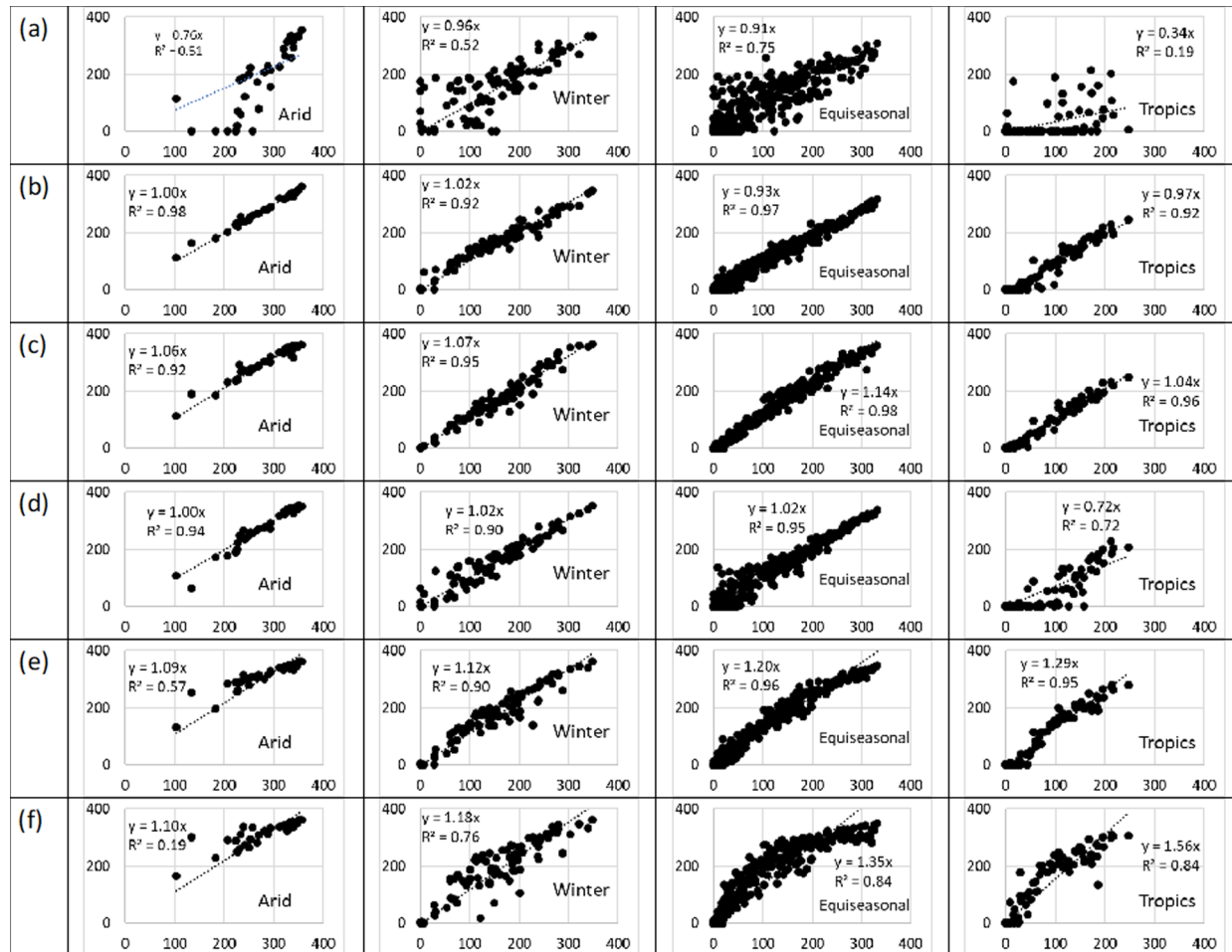


**Fig. 9.** Scatterplots of observed and modelled mean annual ZFD using onsite calibrated parameters for (a) no-transformation (b) log (c) reciprocal (d) square-root (e) one-fifth, and (f) one-tenth transformations in different rainfall regions. x and y axes show observed and modelled ZFDs respectively.

**Table 4**

Regional MKGE of simulated mean annual ZFD for different data transformations using onsite-calibrated (OS), nearest neighbour (NN) and similarity-based (SD) donor parameters.

Rainfall regions = >	Arid			Winter rain			Equisessional			Tropics		
Transformations	OS	NN	SD	OS	NN	SD	OS	NN	SD	OS	NN	SD
No-transformation	-0.7	-1.16	-0.53	0.76	0.56	0.40	0.86	0.73	0.72	-0.5	-0.8	0.30
Log	0.93	0.81	0.54	0.86	0.62	0.53	0.92	0.73	0.76	0.77	0.28	0.37
Reciprocal	0.86	0.79	0.65	0.92	0.61	0.53	0.85	0.80	0.75	0.91	0.35	0.34
Square-root	0.86	0.47	0.62	0.92	0.62	0.53	0.96	0.76	0.77	0.31	0.04	0.38
One-fifth	0.65	0.59	0.66	0.83	0.54	0.49	0.86	0.75	0.69	0.72	0.29	0.22
One-tenth	0.58	0.55	0.65	0.72	0.44	0.39	0.46	0.50	0.40	0.31	0.02	-0.08

**Table 5**

Regional NSE of simulated mean annual ZFD for different data transformations using onsite-calibrated (OS), nearest neighbour (NN) and similarity-based (SD) donor parameters.

Rainfall regions = >	Arid			Winter rain			Equisessional			Tropics		
Transformations	OS	NN	SD	OS	NN	SD	OS	NN	SD	OS	NN	SD
No-transformation	-2.0	-3.3	-2.3	0.52	0.11	-0.06	0.76	0.51	0.49	-0.48	-0.82	-0.94
Log	0.98	0.63	0.03	0.93	0.33	0.18	0.97	0.59	0.58	0.90	-0.57	-0.56
Reciprocal	0.86	0.64	0.30	0.91	0.18	-0.15	0.93	0.57	0.48	0.95	-0.50	-0.72
Square-root	0.92	0.01	0.22	0.90	0.29	0.15	0.94	0.57	0.55	0.55	-0.52	-0.71
One-fifth	0.57	0.44	0.18	0.82	0.05	-0.08	0.87	0.49	0.41	0.71	-0.95	-0.97
One-tenth	0.41	0.39	0.10	0.56	-0.23	-0.38	0.52	0.22	0.03	-0.41	-1.77	-1.72

these transformations enhances lower flows and dampens the higher flows by different extents to overcome the bias shown by goodness-of-fit indicators for high flows while evaluating the objective function during optimisation (Krause et al., 2005). Lower correlation of MKGE between untransformed and reciprocally transformed flows was found

compared to those between untransformed flow and log or square-root transformed flows. This implies that the reciprocal transform changes the flow characteristics more than any other transformation compared to that of the original data and that the MKGE calculation is more sensitive to that transformation (Krause et al. 2005). Pushpalatha et al.

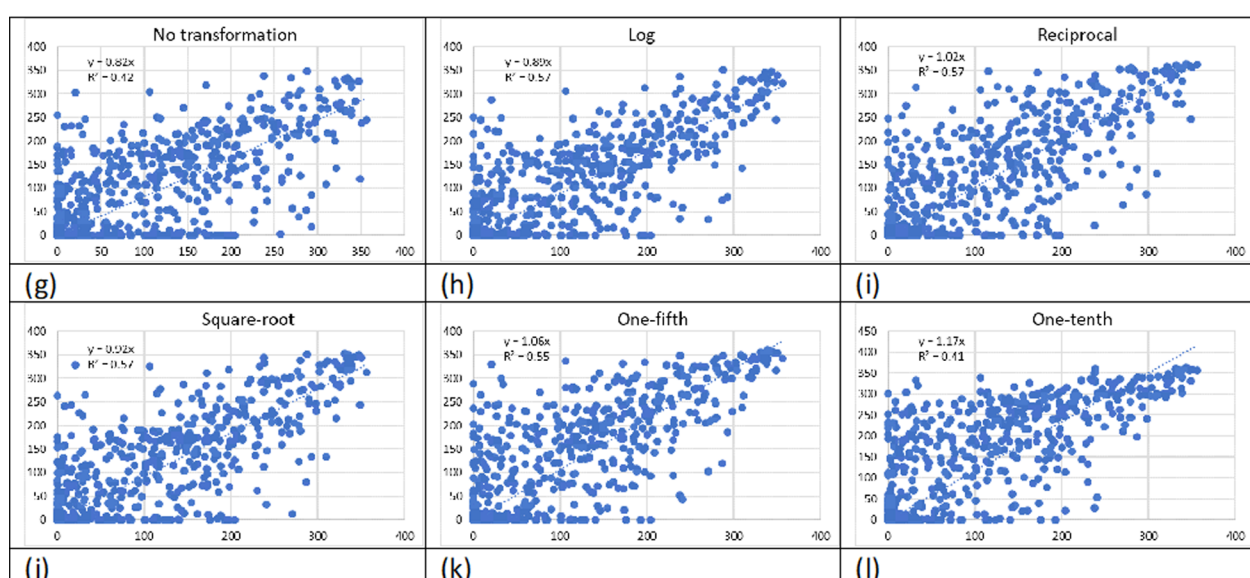
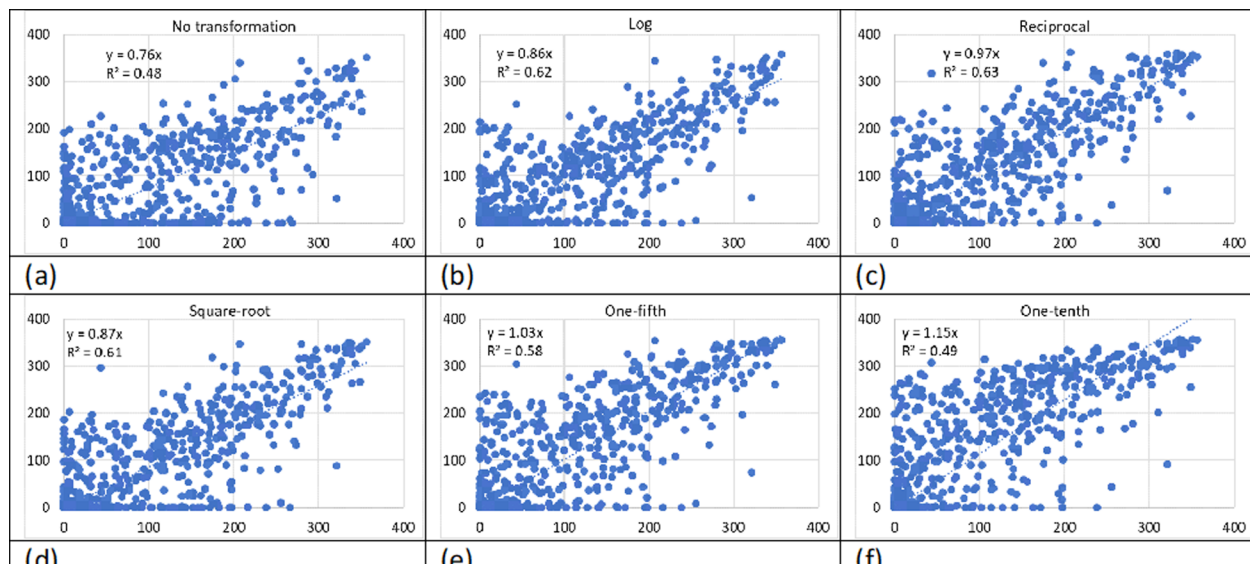


**Fig. 10.** Scatterplots of observed and modelled mean annual ZFDs for different data transformations using donor parameters from nearest neighbour catchments (panels (a)–(f)) and from catchments selected based on the physical similarity criteria (panels (g)–(l)).

**Table 6**

MKGE, NSE and PBIAS of simulated mean annual BFI for different data transformations using onsite-calibrated (OS), nearest neighbour (NN) and similarity-based (SD) parameters. MKGE, NSE and PBIAS of BFI values derived from the regression equation are also shown.

Transformations	MKGE			NSE			PBIAS		
	OS	NN	SD	OS	NN	SD	OS	NN	SD
No-transformation	0.84	0.70	0.63	0.74	0.37	0.21	0.99	-0.19	1.94
Log	0.84	0.68	0.65	0.70	0.44	0.44	-1.91	-2.62	-0.67
Reciprocal	0.70	0.60	0.60	0.44	0.31	0.28	-0.92	-1.29	-0.03
Square-root	0.78	0.73	0.22	0.73	0.44	-0.65	10.90	8.89	12.07
One-fifth	0.47	0.49	0.50	0.15	-0.05	-0.05	5.94	4.40	6.85
One-tenth	0.17	0.28	0.70	-0.47	-0.54	0.37	1.66	0.10	2.17
Regression Equation					0.30				0.0

(2012) mention that the reciprocal transformation tends to focus on the 20% lowest flow on average. As the reciprocal transformation, both enhances the lower flows and dampens the higher flows to a proportionately much larger extent than any other transformations used here, the question whether it serves the purpose of a low flow modelling needs to be resolved based on the objective of the modelling exercise. This suggests that the best transformation for low flow modelling is dependent on the definition of low flow for a given purpose. Therefore, the definition or range of low flow must be established to choose the transformation that serves the range. For example, if near-zero flows

are to be simulated well, then reciprocal transformation may be the best as it gives the highest enhancement of the near-zero flows as described in 4.5.1.

## 6. Summary and conclusion

We studied the impact of different flow transformations on the modelling of lower flow and its surrogates using 595 catchments from different rainfall regions across Australia. The correlation of low flow surrogates, and hydroclimatic variables and catchment characteristics

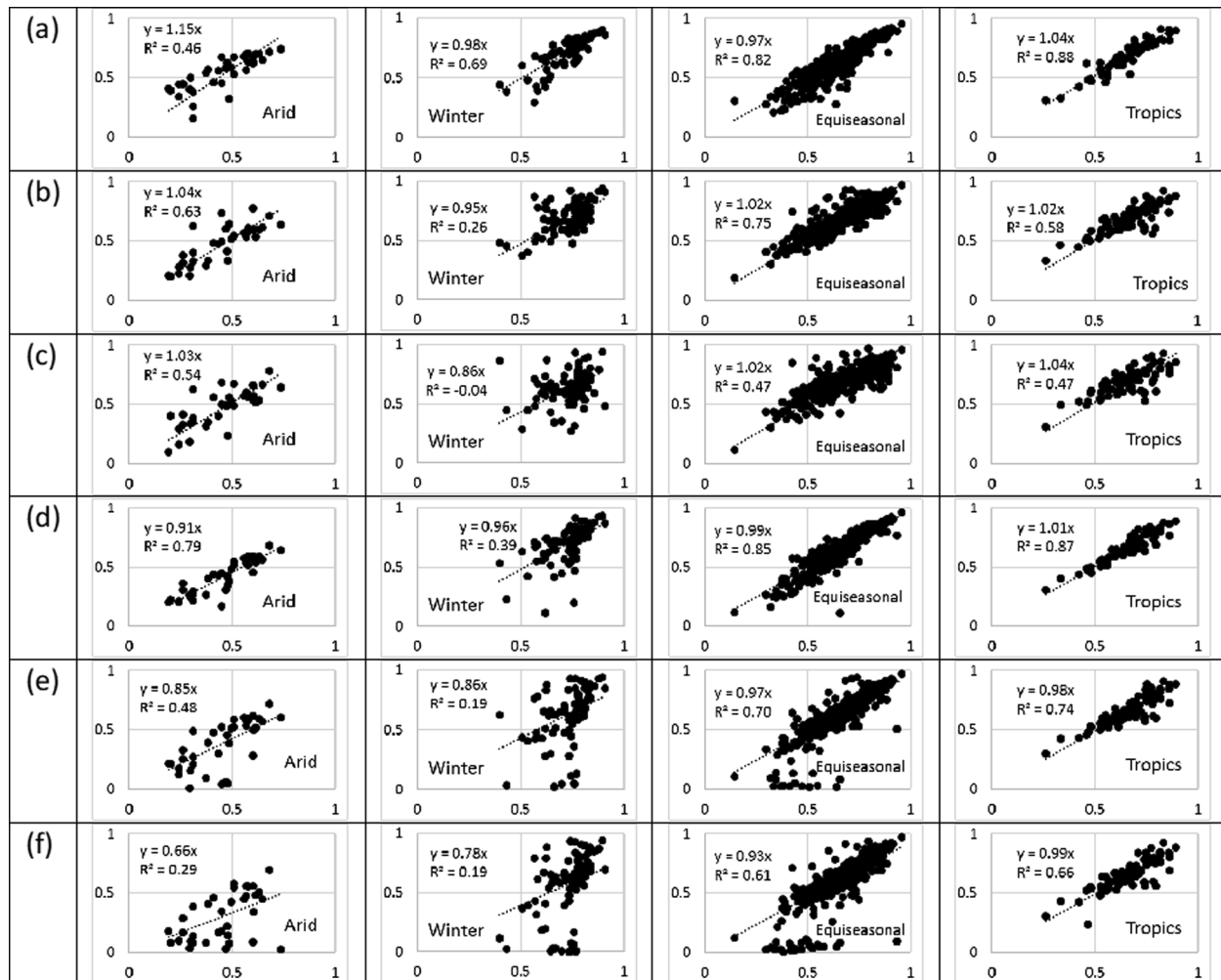


**Fig. 11.** Scatterplots of observed and modelled mean annual baseflow indices using (a) no-transformation (b) log (c) reciprocal (d) square-root (e) one-fifth, and (f) one-tenth transformations.  $\times$  and  $y$  axes show observed and modelled BFIs respectively.

**Table 7**

Regional MKGE values of simulated annual BFI for different data transformations using onsite-calibrated (OS), nearest neighbour (NN) and similarity-based (SD) donor parameters.

Rainfall regions = >	Arid			Winter rain			Equiseasonal			Tropics		
Transformations	OS	NN	SD	OS	NN	SD	OS	NN	SD	OS	NN	SD
No-transformation	0.66	0.58	0.58	0.60	0.31	0.11	0.76	0.69	0.62	0.62	0.71	0.70
Log	0.80	0.67	0.62	0.45	0.17	0.40	0.86	0.71	0.65	0.65	0.61	0.59
Reciprocal	0.75	0.61	0.48	0.023	0.05	-0.03	0.73	0.63	0.64	0.64	0.62	0.53
Square-root	0.82	0.68	0.61	0.25	0.18	0.12	0.77	0.74	0.71	0.71	0.72	0.71
One-fifth	0.26	0.38	0.20	-0.83	-0.83	-0.98	0.53	0.58	0.63	0.63	0.74	0.60
One-tenth	-0.22	-0.09	-0.67	-1.77	-1.71	-1.57	0.30	0.46	0.39	0.62	0.64	0.49

**Table 8**

Regional NSE of simulated annual BFI for different data transformations using onsite-calibrated (OS), nearest neighbour (NN) and similarity-based (SD) donor parameters.

Rainfall regions = >	Arid			Winter rain			Equiseasonal			Tropics		
Transformations	OS	NN	SD	OS	NN	SD	OS	NN	SD	OS	NN	SD
No-transformation	0.24	-0.14	-0.10	0.43	-0.69	-1.42	0.73	0.36	0.18	0.72	0.44	0.34
Log	0.54	0.32	0.15	-0.33	-1.16	-0.76	0.75	0.49	0.44	0.62	0.42	0.46
Reciprocal	0.45	0.27	-0.13	-2.27	-2.27	-2.51	0.58	0.40	0.42	0.48	0.36	0.31
Square-root	0.70	0.34	0.19	-0.61	-1.14	-1.25	0.79	0.47	0.38	0.86	0.50	0.44
One-fifth	-0.23	-0.31	-2.01	-4.68	-5.50	-5.23	0.41	0.19	0.24	0.73	0.50	0.22
One-tenth	-1.53	-0.95	-2.01	-8.60	-9.62	-7.94	-0.04	-0.05	-0.24	0.62	0.32	-0.13

were studied. Performance of three regionalisation techniques, using donor parameters from nearest neighbour catchments and from catchments based on physical similarity criteria together with regression relationships, were evaluated using annual time series and long-term average values of ZFD and BFI. The derived regression relationship estimated the mean annual ZFD well in comparison to the other regionalisation techniques. Estimation of mean annual BFI, however, was better with simulated regionalisation techniques. The effect of the Australian Millennium drought on baseflow in the affected catchments was studied to quantify the changes in baseflow probability during the drought period. We draw the following conclusions:

1. The flow transformations resulting in the best goodness-of-fit did not change for different hydroclimatic regions, rainfall range and extent of forest cover, suggesting that none of the hydroclimatic variables or catchment characteristics influences the transformation type.
2. Most, except very low order transformations, were useful in predicting the long-term mean annual zero flow days and baseflow index. Annual values of ZFD, however, were predicted better with log and reciprocal transformation, while untransformed and square-root performed best for the annual BFI.
3. There was a clear and widespread reduction in the probability of any baseflow in Australia during the millennium drought of 2001–2010. The probabilities were reduced by up to 70% compared to the before drought baseflow probability.
4. The mean annual baseflow index and zero flow (cease-to-flow) days are well correlated with mean annual precipitation and forest cover at a 5% significance level. They are also strongly correlated with each other at a 5% significance level for all rainfall regions.

## Appendix A

The modified KGE is given by

$$\text{MKGE} = 1 - \sqrt{(r - 1)^2 + (\beta - 1)^2 + (\gamma - 1)^2} \quad (\text{A1})$$

5. The statistically significant multiple linear relationships between ZFD and catchment area, precipitation, potential evaporation, catchment slope and forest cover showed precipitation is the biggest influencing factor while the role of the catchment area is relatively insignificant.

## CRediT authorship contribution statement

**Santosh K. Aryal:** Conceptualization, Investigation, Formal analysis, Writing - original draft. **Yongqiang Zhang:** Conceptualization, Writing - review & editing. **Francis Chiew:** Supervision, Writing - review & editing.

## Declaration of Competing Interest

The authors declare that they have no known competing financial interests or personal relationships that could have appeared to influence the work reported in this paper.

## Acknowledgements:

We gratefully acknowledge the constructive comments from anonymous reviewers. We appreciate Junlong Zhang helping to compile some of the time series data for selected catchments. This study was supported by CSIRO strategic project “Low flow hydrological modelling in southeastern Australia”. Yongqiang Zhang acknowledges the support from the CAS Pioneer Hundred Talent Program and the National Natural Science Foundation of China (Grant No. 41971032).

$$\beta = \frac{\mu_s}{\mu_o} \quad (A2)$$

$$\gamma = \frac{CV_s}{CV_o} = \frac{\sigma_s/\mu_s}{\sigma_o/\mu_o} \quad (A3)$$

where  $r$  is correlation coefficient between observed and simulated runoff,  $\beta$  is the bias;  $\gamma$  is variability ratio,  $\mu$  is mean runoff,  $CV$  is coefficient of variation and  $\sigma$  is the standard deviation.  $o$  and  $s$  denote observed and simulated values respectively.

NSE is given by

$$NSE = 1 - \frac{\sum(q_o - q_s)^2}{\sum(q_o - \hat{\mu}_o)^2} \quad (A4)$$

where  $q$  is the runoff.

PBIAS is calculated as

$$PBIAS = \frac{\sum(q_o - q_s)100}{\sum q_o} \quad (A5)$$

## Appendix B. Supplementary data

Supplementary data to this article can be found online at <https://doi.org/10.1016/j.jhydrol.2020.124658>.

## References

- Acreman, M., Dunbar, M., Hannaford, J., Mountford, O., Wood, P., Holmes, N., Cowx, I., Noble, R., Extence, C., Aldrick, J., King, J., Black, A., Crookall, D., 2008. Developing environmental standards for abstractions from UK rivers to implement the EU Water Framework Directive. *Hydrol. Sci. J.* <https://doi.org/10.1623/hysj.53.6.1105>.
- Aguilar, C., Polo, M.J., 2016. Assessing minimum environmental flows in nonpermanent rivers: the choice of thresholds. *Environ. Model. Softw.* <https://doi.org/10.1016/j.envsoft.2016.02.003>.
- Aryal, S.K., Peña Arancibia, J., Viney, N., Yang, A., Wang, B., Hughes, J., Merrin, L., Marvanek, S., Davies, P., Bell, J., Zhang, Y., Vaze, J., Singh, R., Kim, S., 2018. Surface water numerical modelling for the Namoi subregion. Product 2.6.1 for the Namoi subregion from the Northern Inland Catchments Bioregional Assessment. Department of the Environment and Energy, Bureau of Meteorology, CSIRO and Geoscience, Australia, A.
- Australian Bureau of Meteorology, 2015. Recent rainfall, drought and southern Australia's long-term rainfall decline [WWW Document]. URL <http://www.bom.gov.au/climate/updates/articles/a010-southern-rainfall-decline.shtml>. (Accessed 7. 12.19).
- Bates, B.C., Aryal, S.K., 2014. A similarity index for storm runoff due to saturation excess overland flow. *J. Hydrol.* 513, 241–255. <https://doi.org/10.1016/j.jhydrol.2014.03.021>.
- Bloomfield, J.P., Allen, D.J., Griffiths, K.J., 2009. Examining geological controls on baseflow index (BFI) using regression analysis: an illustration from the Thames Basin. *J. Hydrol.* <https://doi.org/10.1016/j.jhydrol.2009.04.025>.
- Brown, A.E., Western, A.W., McMahon, T.A., Zhang, L., 2013. Impact of forest cover changes on annual streamflow and flow duration curves. *J. Hydrol.* <https://doi.org/10.1016/j.jhydrol.2012.12.031>.
- Burn, D.H., Boorman, D.B., 1993. Estimation of hydrological parameters at ungauged catchments. *J. Hydrol.* [https://doi.org/10.1016/0022-1694\(93\)90203-L](https://doi.org/10.1016/0022-1694(93)90203-L).
- Caruso, B.S., 2002. Temporal and spatial patterns of extreme low flows and effects on stream ecosystems in Otago, New Zealand. *J. Hydrol.* [https://doi.org/10.1016/S0022-1694\(01\)00546-7](https://doi.org/10.1016/S0022-1694(01)00546-7).
- Chapman, T., 1999. A comparison of algorithms for stream flow recession and baseflow separation. *Hydrol. Process.* [https://doi.org/10.1002/\(SICI\)1099-1085\(19990415\)13:5<701::AID-HYP774>3.0.CO;2-2](https://doi.org/10.1002/(SICI)1099-1085(19990415)13:5<701::AID-HYP774>3.0.CO;2-2).
- Chiew, F.H.S., Siriwardena, L., 2005. Estimation of SIMHYD parameter values for application in ungauged catchments. In: MODSIM 2005 International Congresson Modelling and Simulation. Modelling and Simulation Society of Australia and New Zealand, pp. 2883–2889. <[http://www.mssanz.org.au/modsim05/papers/chiew\\_2.pdf](http://www.mssanz.org.au/modsim05/papers/chiew_2.pdf)>
- Chiew, F.H.S., Stewardson, M.J., McMahon, T.A., 1993. Comparison of six rainfall-runoff modelling approaches. *J. Hydrol.* [https://doi.org/10.1016/0022-1694\(93\)90073-I](https://doi.org/10.1016/0022-1694(93)90073-I).
- Cleff, T., 2014. Exploratory data analysis in business and economics. *Explor. Data Anal. Business Econ.* <https://doi.org/10.1007/978-3-319-01517-0>.
- Corder, G.W., Foreman, D.I., 2009. Nonparametric statistics: an introduction. *Nonparametric Stat. Non-Statisticians A Step-by-Step Approach* 1–11. <https://doi.org/10.1002/9781118165881.ch1>.
- Coron, L., Andréassian, V., Perrin, C., Lerat, J., Vaze, J., Bourqui, M., Hendrickx, F., 2012. Crash testing hydrological models in contrasted climate conditions: an experiment on 216 Australian catchments. *Water Resour. Res.* <https://doi.org/10.1029/2011WR011721>.
- De Vera, M.R., 1984. Rainfall-runoff relationship of some catchments with karstic geomorphology under arid to semi-arid conditions. *J. Hydrol.* [https://doi.org/10.1016/0022-1694\(84\)90205-1](https://doi.org/10.1016/0022-1694(84)90205-1).
- Duan, Q., Sorooshian, S., Gupta, V.K., 1994. Optimal use of the SCE-UA global optimization method for calibrating watershed models. *J. Hydrol.* [https://doi.org/10.1016/0022-1694\(94\)90057-4](https://doi.org/10.1016/0022-1694(94)90057-4).
- Eckhardt, K., 2005. How to construct recursive digital filters for baseflow separation. *Process. Hydrol.* <https://doi.org/10.1002/hyp.5675>.
- Eckhardt, K., 2008. A comparison of baseflow indices, which were calculated with seven different baseflow separation methods. *J. Hydrol.* <https://doi.org/10.1016/j.jhydrol.2008.01.005>.
- Eckhardt, K., Arnold, J.G., 2001. Automatic calibration of a distributed catchment model. *J. Hydrol.* [https://doi.org/10.1016/S0022-1694\(01\)00429-2](https://doi.org/10.1016/S0022-1694(01)00429-2).
- Efstratiadis, A., Tegos, A., Varveris, A., Koutsoyiannis, D., 2014. Assessment of environmental flows under limited data availability: case study of the Acheloos River. *Hydrolog. Sci. J.* <https://doi.org/10.1080/02626667.2013.804625>.
- Gupta, H.V., Kling, H., Yilmaz, K.K., Martinez, G.F., 2009. Decomposition of the mean squared error and NSE performance criteria: implications for improving hydrological modelling. *J. Hydrol.* <https://doi.org/10.1016/j.jhydrol.2009.08.003>.
- Hamel, P., Guswa, A.J., Sahl, J., Zhang, L., 2017. Predicting dry-season flows with a monthly rainfall-runoff model: performance for gauged and ungauged catchments. *Process. Hydrol.* <https://doi.org/10.1002/hyp.11298>.
- Hannaford, J., Marsh, T., 2006. An assessment of trends in UK runoff and low flows using a network of undisturbed catchments. *J. Climatol. Int.* <https://doi.org/10.1002/joc.1303>.
- Hauke, J., Kossowski, T., 2011. Comparison of values of pearson's and spearman's correlation coefficients on the same sets of data. *Geogr. Quaest.* <https://doi.org/10.2478/v10117-011-0021-1>.
- Kling, H., Fuchs, M., Paulin, M., 2012. Runoff conditions in the upper Danube basin under an ensemble of climate change scenarios. *J. Hydrol.* <https://doi.org/10.1016/j.jhydrol.2012.01.011>.
- Krause, P., Boyle, D.P., Bäse, F., 2005. Comparison of different efficiency criteria for hydrological model assessment. *Geosci. Adv.* <https://doi.org/10.5194/adgeo-5-89-2005>.
- Laaha, G., Blöschl, G., 2006. A comparison of low flow regionalisation methods-catchment grouping. *J. Hydrol.* <https://doi.org/10.1016/j.jhydrol.2005.09.001>.
- Lacey, G.C., Grayson, R.B., 1998. Relating baseflow to catchment properties in south-eastern Australia. *J. Hydrol.* [https://doi.org/10.1016/S0022-1694\(97\)00124-8](https://doi.org/10.1016/S0022-1694(97)00124-8).
- Larned, S.T., Datry, T., Arscott, D.B., Tockner, K., 2010. Emerging concepts in temporary-river ecology. *Freshwater Biol.* <https://doi.org/10.1111/j.1365-2427.2009.02322.x>.
- Li, F., Zhang, Y., Xu, Z., Teng, J., Liu, C., Liu, W., Mpelasoka, F., 2013. The impact of climate change on runoff in the southeastern Tibetan Plateau. *J. Hydrol.* <https://doi.org/10.1016/j.jhydrol.2013.09.052>.
- Li, M., Shao, Q., Zhang, L., Chiew, F.H.S., 2010. A new regionalization approach and its application to predict flow duration curve in ungauged basins. *J. Hydrol.* <https://doi.org/10.1016/j.jhydrol.2010.05.039>.
- Lyne, V.D., Hollick, M., 1979. Stochastic time-variable rainfall runoff modelling. In: *Hydrology and Water Resources Symposium*. Institution of Engineers, Australia, Perth, pp. 89–92.
- McCuen, R.H., Knight, Z., Cutter, A.G., 2006. Evaluation of the Nash-Sutcliffe Efficiency Index. *J. Hydrol. Eng.* [https://doi.org/10.1061/\(ASCE\)1084-0699\(2006\) 11:6\(597\)](https://doi.org/10.1061/(ASCE)1084-0699(2006) 11:6(597)).
- McIntyre, N., Al-Qurashi, A., Wheater, H., 2007. Regression analysis of rainfall-runoff data from an arid catchment in Oman. *Hydrol. Sci. J.* 52, 1103–1118. <https://doi.org/10.1080/02626667.2007.9514532>.
- Merz, R., Blöschl, G., 2009. A regional analysis of event runoff coefficients with respect to climate and catchment characteristics in Austria. *Water Resour. Res.* <https://doi.org/10.1029/2008WR007163>.
- Merz, R., Blöschl, G., 2004. Regionalisation of catchment model parameters. *J. Hydrol.* <https://doi.org/10.1016/j.jhydrol.2003.09.028>.

- Nepal, S., Chen, J., Penton, D.J., Neumann, L.E., Zheng, H., Wahid, S., 2017. Spatial GR4J conceptualization of the Tamor glaciated alpine catchment in Eastern Nepal: evaluation of GR4JSG against streamflow and MODIS snow extent. *Hydrol. Process.* 31, 51–68. <https://doi.org/10.1002/hyp.10962>.
- Nicolle, P., Pushpalatha, R., Perrin, C., François, D., Thiéry, D., Mathevet, T., Le Lay, M., Besson, F., Soubeyroux, J.M., Viel, C., Regimbeau, F., Andréassian, V., Maugis, P., Augeard, B., Morice, E., 2014. Benchmarking hydrological models for low-flow simulation and forecasting on French catchments. *Hydrol. Earth Syst. Sci.* <https://doi.org/10.5194/hess-18-2829-2014>.
- Oudin, L., Andréassian, V., Mathevet, T., Perrin, C., Michel, C., 2006. Dynamic averaging of rainfall-runoff model simulations from complementary model parameterizations. *Water Resour. Res.* <https://doi.org/10.1029/2005WR004636>.
- Parajka, J., Merz, R., Blöschl, G., 2005. A comparison of regionalisation methods for catchment model parameters. *Hydrol. Earth Syst. Sci.* <https://doi.org/10.5194/hess-9-157-2005>.
- Perrin, C., Michel, C., Andréassian, V., 2003. Improvement of a parsimonious model for streamflow simulation. *J. Hydrol.* 279, 275–289. [https://doi.org/10.1016/S0022-1694\(03\)00225-7](https://doi.org/10.1016/S0022-1694(03)00225-7).
- Price, K., 2011. Effects of watershed topography, soils, land use, and climate on baseflow hydrology in humid regions: a review. *Prog. Phys. Geogr.* <https://doi.org/10.1177/0309133111402714>.
- Pushpalatha, R., Perrin, C., Le Moine, N., Andréassian, V., 2012. A review of efficiency criteria suitable for evaluating low-flow simulations. *J. Hydrol.* <https://doi.org/10.1016/j.jhydrol.2011.11.055>.
- Rolls, R.J., Leigh, C., Sheldon, F., 2012. Mechanistic effects of low-flow hydrology on riverine ecosystems: ecological principles and consequences of alteration. *Freshw. Sci.* <https://doi.org/10.1899/12-002.1>.
- Schaefli, B., Gupta, H.V., 2007. Do Nash values have value? *Hydrol. Process.* <https://doi.org/10.1002/hyp.6825>.
- Shapiro, S.S., Wilk, M.B., 1965. An Analysis of Variance Test for Normality (Complete Samples). *Biometrika*. <https://doi.org/10.2307/2333709>.
- Sheldon, F., 2017. Characterising the ecological effects of changes in the ‘low-flow hydrology’ of the Barwon-Darling River: Advice to the Commonwealth Environmental Water Holder Office.
- Smakhtin, V.U., 2001. Low flow hydrology: a review. *J. Hydrol.* [https://doi.org/10.1016/S0022-1694\(00\)00340-1](https://doi.org/10.1016/S0022-1694(00)00340-1).
- Staudinger, M., Stahl, K., Seibert, J., Clark, M.P., Tallaksen, L.M., 2011. Comparison of hydrological model structures based on recession and low flow simulations. *Hydrol. Earth Syst. Sci.* <https://doi.org/10.5194/hess-15-3447-2011>.
- Stromberg, J.C., Beauchamp, V.B., Dixon, M.D., Lite, S.J., Paradzick, C., 2007. Importance of low-flow and high-flow characteristics to restoration of riparian vegetation along rivers in arid south-western United States. *Freshw. Biol.* <https://doi.org/10.1111/j.1365-2427.2006.01713.x>.
- Xiao, C., Ye, J., Esteves, R.M., Rong, C., 2016. Using Spearman’s correlation coefficients for exploratory data analysis on big dataset. In: Concurrency Computation, <https://doi.org/10.1002/cpe.3745>.
- Zhang, J., Zhang, Y., Song, J., Cheng, L., Gan, R., Shi, X., Luo, Z., Zhao, P., 2017. Comparing hydrological modelling, linear and multilevel regression approaches for predicting baseflow index for 596 catchments across Australia. *Hydrol. Earth Syst. Sci. Discuss.* <https://doi.org/10.5194/hess-2017-737>.
- Zhang, Y., Ahiablame, L., Engel, B., Liu, J., 2013. Regression modeling of baseflow and baseflow index for Michigan USA. *Water (Switzerland)*. <https://doi.org/10.3390/w5041797>.
- Zhang, Y., Chiew, F.H.S., 2009. Relative merits of different methods for runoff predictions in ungauged catchments. *Water Resour. Res.* <https://doi.org/10.1029/2008WR007504>.
- Zhang, Y., Chiew, F.H.S., Li, M., Post, D., 2018. Predicting Runoff Signatures Using Regression and Hydrological Modeling Approaches. *Water Resour. Res.* <https://doi.org/10.1029/2018WR023325>.
- Zhang, Y., Vaze, J., Chiew, F.H.S., Teng, J., Li, M., 2014. Predicting hydrological signatures in ungauged catchments using spatial interpolation, index model, and rainfall-runoff modelling. *J. Hydrol.* <https://doi.org/10.1016/j.jhydrol.2014.06.032>.